Progress of Theoretical Physics, Vol. 60, No. 3, September 1978

Textures in Rotating Superfluid ^{3}He-A

Toshimitsu FUJITA, Mikio NAKAHARA,*
Tetsuo OHMI* and Toshihiko TSUNETO*

Department of Physics, Wakayama University, Wakayama 640
**Department of Physics, Kyoto University, Kyoto 606*

(Received March 9, 1978)

Possible textures in the rotating superfluid ^{3}He-A are studied in the London limit. Three types of textures without singular cores, i.e., the non-singular vortex lattice, the vortex-sheet lattice and the concentric sheet structure, are explicitly constructed. The estimate of the free energy associated with each structure is made and the results indicate the first type is most stable.

§ 1. Introduction

In view of unusual properties as a superfluid[1] it is interesting to see what will happen to the superfluid ^{3}He in its A phase when rotated. In an equilibrium state any fluid in a rotating bucket must make rigid body rotation as a whole. This is achieved in the case of the superfluid ^{4}He by having a lattice of quantized vortex lines;[2] vorticity resides, so to speak, only at their singular cores where the superfluid order parameter vanishes. While it is possible, just as in ^{4}He-II, to have a lattice of ordinary vortex lines in a uniform textures, one would naturally like to ask whether or not a lattice can be formed of the so-called Mermin-Ho (M-H)[3] or Anderson-Toulouse (A-T)[4] structures since these linear structures support vorticity diffusely by bending of the l-vector and hence have no singular core. Volovik and Kopnin[5] discussed this problem and suggested a lattice of A-T structures as a possibility. In a preliminary report[6] we presented an explicit form of a lattice of the linear structures without singular cores together with other possibilities.

The purpose of the present work is to study this problem in more details. In the next section we give the expressions of the relevant free energy and current density in terms of the order parameters for ^{3}He-A in a rotating bucket near T_c. In § 3 we present as possible states of the rotating superfluid the three types of structures, a lattice of ordinary vortex lines, that of the M-H or A-T structures, and structures characterized by sheets of discontinuity in the phase functions of the order parameters. In § 4 we try to estimate the free energy of these states. In the main part of the work we assume that the container is a cylinder of large size and neglect the boundary condition at the wall. This as well as the effect of magnetic field will be discussed in the last section.

§ 2. Free energy of the rotating superfluid

As is well known, the superfluid states of ^{3}P-pairing are described by the condensation amplitudes

$$\Delta_{\alpha\beta}=i|\Delta|A_{\mu i}\hat{k}_i(\sigma_\mu\sigma_2)_{\alpha\beta}, \tag{2·1}$$

where μ, $i=x\,y\,z$ and $\sum_{\mu i}|A_{\mu i}|^2=1$. In particular the A-phase is identified as a class of states called ABM states with the order parameter of the form

$$A_{\mu i}=\frac{1}{\sqrt{2}}\hat{d}_\mu(\hat{\Delta}_{1i}+i\hat{\Delta}_{2i}), \tag{2·2}$$

where $\hat{\boldsymbol{d}}$, $\hat{\boldsymbol{\Delta}}_1$ and $\hat{\boldsymbol{\Delta}}_2$ are real unit vectors and $\hat{\boldsymbol{\Delta}}_1$, $\hat{\boldsymbol{\Delta}}_2$ and $\hat{\boldsymbol{\Delta}}_1\times\hat{\boldsymbol{\Delta}}_2\equiv\hat{\boldsymbol{l}}$ form a triad that represents the orbital state of the pair. Throughout this work we take the London limit, assuming spatial variations to be slow, in other words, we assume that non-uniform states are described by the fields of $\hat{\boldsymbol{d}}$ vector and the triad, the condensation energy and hence $|\Delta|$ being kept constant.

Since we take the London limit, we have to consider only the derivative terms in the free energy. For simplicity we adopt their expression valid near T_c in the weak coupling limit:

$$f=\frac{\rho_{s\parallel}}{(2m)^2}(\partial_iA^*_{\mu i}\partial_jA_{\mu j}+\partial_iA^*_{\mu j}\partial_iA_{\mu j}+\partial_iA^*_{\mu j}\partial_jA_{\mu i}). \tag{2·3}$$

In our problem it is convenient to use the frame of reference rotating with the container. Starting with the microscopic Hamiltonian $H-L\cdot\Omega$ where L is the total angular momentum operator, we can rewrite it as $\mathcal{H}(\boldsymbol{A})-(m/2)\int\psi^\dagger(\boldsymbol{\Omega}\times\boldsymbol{r})^2\psi\,d\boldsymbol{r}$ with the vector potential $\boldsymbol{A}=m(\boldsymbol{\Omega}\times\boldsymbol{r})$ and absorb the second term in the local chemical potential. Therefore, invoking the gauge invariance we obtain the relevant free energy in the rotating frame merely by replacing ∂_i by $(\partial_i-2im(\boldsymbol{\Omega}\times\boldsymbol{r})_i)$ in (2·3).

Minimizing this free energy is equivalent to minimizing $F-L\cdot\Omega$ where L is the sum of the angular momentum of the superfluid and that of the normal fluid. Even on the assumption that the normal fluid is at rest in the rotating frame, we should not use just L_s because L_n depends on the texture.

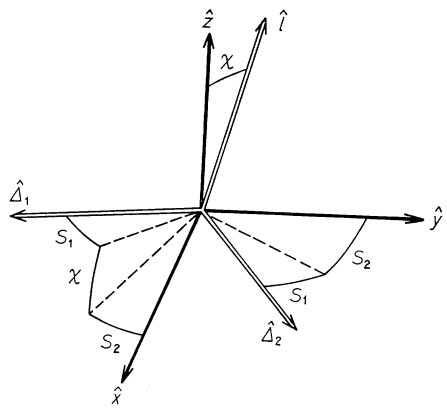

Fig. 1. The Euler angles S_1, S_2 and χ.

Similarly, the current density in the rotating frame is obtained from

$$j_i=\frac{\rho_{s\parallel}}{m}\mathrm{Im}(A^*_{\mu i}\partial_jA_{\mu j}+A^*_{\mu j}\partial_iA_{\mu j}+A^*_{\mu j}\partial_jA_{\mu i}) \tag{2·4}$$

by the same replacement. In what follows we always use the rotating frame of reference unless stated otherwise.

In the A-phase the triad at any point can be specified by the Euler angles (S_1, χ, S_2) the rotation with which brings the standard frame $(\hat{\boldsymbol{x}}, \hat{\boldsymbol{y}}, \hat{\boldsymbol{z}})$ to the triad (Fig. 1). In terms of these angles we have

$$(\hat{\boldsymbol{\Delta}}_1 + i\hat{\boldsymbol{\Delta}}_2) = e^{iS_1}(\hat{\boldsymbol{m}} + i\hat{\boldsymbol{n}}), \tag{2·5}$$

$$\hat{\boldsymbol{m}} = \begin{pmatrix} \cos\chi\cos S_2 \\ -\cos\chi\sin S_2 \\ \sin\chi \end{pmatrix}, \quad \hat{\boldsymbol{n}} = \begin{pmatrix} \sin S_2 \\ \cos S_2 \\ 0 \end{pmatrix} \tag{2·6}$$

and

$$\hat{\boldsymbol{l}} = \begin{pmatrix} -\sin\chi\cos S_2 \\ \sin\chi\sin S_2 \\ \cos\chi \end{pmatrix}. \tag{2·7}$$

In the following discussion it is sometimes convenient to use the representation of the order parameters $\hat{\boldsymbol{\Delta}}_1 + i\hat{\boldsymbol{\Delta}}_2 = \sum_{m=-1}^{1} \psi_m \hat{\boldsymbol{e}}_m$ with the basis $\hat{\boldsymbol{e}}_{\pm 1} = 1/\sqrt{2}\,(\hat{\boldsymbol{x}} \pm i\hat{\boldsymbol{y}})$ and $\hat{\boldsymbol{e}}_0 = \hat{\boldsymbol{z}}$:

$$\begin{aligned} \psi_1 &= \frac{1}{\sqrt{2}} e^{i(S_1+S_2)}(1+\cos\chi), \\ \psi_0 &= e^{iS_1}\sin\chi, \\ \psi_{-1} &= -\frac{1}{\sqrt{2}} e^{i(S_1-S_2)}(1-\cos\chi). \end{aligned} \tag{2·8}$$

For later use we write down the free energy in terms of the Euler angles in the case where d-vector is locked to l-vector, in other words, spatial variations occur over a scale large compared to the dipole coherence length. In this case the free energy is split into two parts $f_{\rm sp}$ and $f_{\rm orb}$, coming from the derivatives of $\hat{\boldsymbol{d}}$ and $(\hat{\boldsymbol{\Delta}}_1 + i\hat{\boldsymbol{\Delta}}_2)$, respectively:

$$f = f_{\rm sp} + f_{\rm orb},$$

$$\begin{aligned} f_{\rm sp} = \frac{\rho_{s\parallel}}{(2m)^2}\{&2(\hat{\boldsymbol{m}}\cdot\boldsymbol{\nabla}\chi)^2 + 2(\sin\chi\,\hat{\boldsymbol{n}}\cdot\boldsymbol{\nabla}S_2)^2 \\ &+ 2(\hat{\boldsymbol{n}}\cdot\boldsymbol{\nabla}\chi)^2 + 2(\sin\chi\,\hat{\boldsymbol{m}}\cdot\boldsymbol{\nabla}S_2)^2 \\ &+ (\hat{\boldsymbol{l}}\cdot\boldsymbol{\nabla}\chi)^2 + \sin^2\chi(\hat{\boldsymbol{l}}\cdot\boldsymbol{\nabla}S_2)^2\}, \end{aligned} \tag{2·9}$$

$$\begin{aligned} f_{\rm orb} = \frac{\rho_{s\parallel}}{2(2m)^2}\{&2(\boldsymbol{v}\cdot\hat{\boldsymbol{m}} - \sin\chi\,\hat{\boldsymbol{l}}\cdot\boldsymbol{\nabla}S_2)^2 \\ &+ 2(\boldsymbol{v}\cdot\hat{\boldsymbol{n}} - \hat{\boldsymbol{l}}\cdot\boldsymbol{\nabla}\chi)^2 \\ &+ (\boldsymbol{v} - \hat{\boldsymbol{m}}\times\boldsymbol{\nabla}\chi)^2 + (\boldsymbol{v} + \sin\chi\,\hat{\boldsymbol{n}}\times\boldsymbol{\nabla}S_2)^2 \\ &+ (\hat{\boldsymbol{m}}\cdot\boldsymbol{\nabla}\chi)^2 + \sin^2\chi(\hat{\boldsymbol{n}}\cdot\boldsymbol{\nabla}S_2)^2\}, \end{aligned} \tag{2·10}$$

where we have defined

$$\begin{aligned} \boldsymbol{v} &\equiv 2m\boldsymbol{v}_s = \Delta_{1i}\nabla\Delta_{2i} - \boldsymbol{\omega}\times\boldsymbol{r} \\ &= \cos\chi\nabla S_2 + (\nabla S_1 - \boldsymbol{\omega}\times\boldsymbol{r}) \end{aligned} \tag{2·11}$$

with $\boldsymbol{\omega} = 2m\boldsymbol{\Omega}$ ($= 2\pi\boldsymbol{\Omega}/\kappa$, κ being the quantum of circulation of the pair, $h/2m$). Since the derivatives of $\hat{\boldsymbol{d}}$ do not contribute to the current density, we find

$$\begin{aligned} \boldsymbol{j} = \frac{\rho_{s\parallel}}{2m}\{&4\boldsymbol{v} - \boldsymbol{m}\sin\chi(\boldsymbol{l}\cdot\nabla S_2) - \boldsymbol{n}(\boldsymbol{l}\cdot\nabla\chi) \\ &- \boldsymbol{l}[\boldsymbol{n}\cdot\nabla\chi + \sin\chi(\boldsymbol{m}\cdot\nabla S_2) + 2\boldsymbol{l}\cdot\boldsymbol{v}]\}. \end{aligned} \tag{2·12}$$

We note that $\rho_{s\parallel}$ here is the superfluid density for one spin component.

§ 3. Textures of the rotating superfluid

We now consider the superfluid in a large cylinder with radius R. In general, if the system does not perform rigid body rotation as a whole, a term proportional to R^4 appears in the total free energy in the rotating frame. Extracting the common phase of the order parameters as $e^{iS}A_{\mu i}$, we can avoid having such a term if the function S behaves in such a way that

$$\partial_x S \sim -\omega y\,, \quad \partial_y S \sim \omega x\,. \tag{3·1}$$

In the case of the A phase this is clear from the combination $(\nabla S_1 - \boldsymbol{\omega}\times\boldsymbol{r})$ in (2·10) and (2·11) (obviously $S = S_1$).[5] Now, there are various possibilities in choosing the function S_1 satisfying the condition (3·1).

[a] *Lattice structures*

An obvious possibility is to use S_1 similar to the phase functions describing vortex lattices in the ordinary superfluid. Let $\boldsymbol{\omega} = \omega\hat{\boldsymbol{z}}$ and consider a lattice whose lattice points are given by

$$(X_{mn}, Y_{mn}) = (ma + nb\cos\alpha, nb\sin\alpha). \tag{3·2}$$

Within the unit cell (m, n) we introduce the coordinates (x_0, y_0) such that

$$\begin{aligned} x &= X_{mn} + x_0\,, \\ y &= Y_{mn} + y_0\,. \end{aligned} \tag{3·3}$$

In order that $\boldsymbol{v}$ defined by (2·11) and hence the free energy density become periodic functions with the same symmetry as the lattice, it is necessary that S_1 satisfies

$$\begin{aligned} S_1(x, y) = S_1(x_0, y_0) &+ \omega X_{mn} y_0 \\ &- \omega Y_{mn} x_0 + C_{mn}\,, \end{aligned} \tag{3·4}$$

where C_{mn} is a constant necessary for making S_1 continuous at the cell boundary.

Indeed we then have $\nabla S_1 - \boldsymbol{\omega} \times \boldsymbol{r} = \nabla_0 S_1 - \boldsymbol{\omega} \times \boldsymbol{r}_0$. To satisfy the condition (3·4) S_1 must have a set of singular points and/or singular lines with the same translational symmetry as the lattice. In general, the function S_1 with point singularity at each lattice site L can be expressed as

$$S_1 = \Phi_L + S_1' , \tag{3·5}$$

where S_1' is an analytic function of the lattice symmetry and Φ_L is the phase function of the lattice of vortex lines in the ordinary superfluid satisfying (3·4). Since Φ_L increases by $2\omega ab \sin\alpha$ as we go around each lattice point, we have

$$2\omega ab \sin\alpha = 2p\pi \tag{3·6}$$

with positive integer p, relating the unit cell area with ω. If we choose such S_1, the free energy becomes the sum of that in one unit cell. Consequently, to determine the equilibrium states we have to find S_1', S_2 and χ (and subsequently the lattice parameters) which minimize this free energy per unit cell. We remark that this procedure is valid not only for the A phase but for a general case of ^{3}P pairing (the common phase S of A_{ij} plays the role of S_1 as remarked before).

Since it is extremely difficult to solve the minimization problem, we proceed by constructing various types of the possible structures.

[a.1] Lattice of vortex lines with a singular core

The simplest structure is, of course, the lattice of ordinary vortex lines in a uniform texture, which corresponds to $\chi = \text{const}$ and $S_2 = \text{const}$. Without loss of generality we put $S_2 = 0$. In this case we can find S_1 which minimizes the free energy,

$$F_{\text{crb}} = \frac{\rho_{s\parallel}}{(2m)^2} \int_{\text{cell}} [(1+\cos^2\chi)\,(\partial_x S_1 + \omega y)^2 + 2(\partial_y S_1 - \omega x)^2]\, dx dy . \tag{3·7}$$

After scale transformation[7]

$$x = \left(\frac{1+\cos^2\chi}{2}\right)^{1/4} X , \quad y = \left(\frac{2}{1+\cos^2\chi}\right)^{1/4} Y \tag{3·8}$$

it becomes

$$F_{\text{orb}} = \frac{\rho_{s\parallel}\sqrt{2(1+\cos^2\chi)}}{(2m)^2} \int_{\text{cell}} [(\partial_X S_1 + \omega Y)^2 + (\partial_Y S_1 - \omega X)^2]\, dX dY . \tag{3·9}$$

The variation with respect to S_1 gives $(\partial_X^2 + \partial_Y^2) S_1 = 0$ so that the problem is identical to that of a vortex lattice in an ideal fluid. Hence, in the transformed coordinates S_1 becomes Φ_L itself. The complex potential defined by

$$\zeta_0(X+iY) = (\partial_Y \Phi_L + i\partial_X \Phi_L) \tag{3·10}$$

is given by the Weierstrass ζ-function, and according to Tkachenko[2] the triangular

lattice with $p=1$ is most stable. From (3·9) the energy is lowest when $\chi=\pi/2$, that is, when $\hat{\boldsymbol{l}} \perp \boldsymbol{\Omega}$ everywhere. In the original coordinates the lattice is elongated in the y (or x) direction, and its energy is lowered because $\rho_{s\parallel}<\rho_{s\perp}$.

It is appropriate to remark here that, although the lattice, and hence the superfluid, always makes the rigid body rotation as a whole, the total angular momentum of the superfluid obviously varies with the orientation of $\hat{\boldsymbol{l}}$ vector. The total angular momentum of the normal and the superfluid, however, is always the same. This remark applies in general to any structure under consideration.

[a·2] Non-singular lattice—Type I

We now remove the singular cores of the above vortex lattice by making use of the remaining freedom in the order parameters.

From the representation (2·8) we see that where $\chi=0$ (π) the singularity of the vortex type in the phase function S_1-S_2 (S_1+S_2) does not lead to divergent $\boldsymbol{v}$ provided S_1+S_2 (S_1-S_2) is analytic. This suggests, as we explained in a previous report,[6] the following lattice structure. We choose two sets of lattice sites $\{L\}$ and $\{C\}$ where $\chi=0$ and π, that is, $\hat{\boldsymbol{l}}=\hat{\boldsymbol{z}}$ and $-\hat{\boldsymbol{z}}$, respectively, and suppose

$$S_1=\Phi_C+\Phi_L+S_1',$$
$$S_2=\Phi_C-\Phi_L+S_2', \tag{3·11}$$

where Φ_L and Φ_C are the phase functions of vortex lattices having branch points at L and C sites, respectively, and S_1' and S_2' are analytic functions of the lattice periodicity. Here Φ_L and Φ_C satisfy the condition (3·4) with $\omega/2$ instead of ω. Consequently, we have

$$\omega ab \sin\alpha=2p\pi. \tag{3·12}$$

As we have said before, S_1', S_2' and χ should be determined by the free energy minimum. It must be remarked that, in order for the velocity $\boldsymbol{v}$ to vanish at both L and C sites in the rotating frame, one set of the lattice sites must be situated at the points where the velocity due to another lattice vanishes. In the following we call this type of structure the non-singular type I lattice. As an example of the resulting lattice structures, we reproduce in Fig. 2 the triad configuration given previously.[6]

[a·3] Non-singular lattice—Type II

Instead of having the two sets of lattice points, we can stretch the phase discontinuity, say, at the C-sites into a sheet (a line in x-y plane) of discontinuity surrounding the L-sites (Fig. 3(a)). In other words the phase S_1+S_2 slips along this sheet where $\chi=\pi$. More explicitly we take in the (m,n)-th cell

$$S_1+S_2=2\Phi_L^{(m,n)}, \tag{3·13}$$

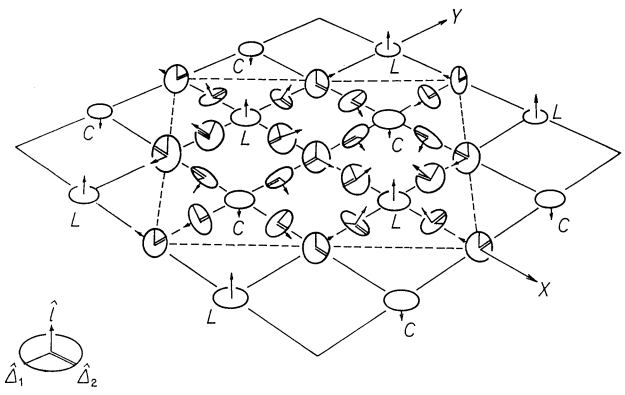

Fig. 2. The configuration of the order parameter without the common phase factor e^{iS_1} in the type I lattice. The numbers 1, 2 and 3 label the unit vector $\hat{\boldsymbol{\Delta}}_1$, $\hat{\boldsymbol{\Delta}}_2$ and $\hat{\boldsymbol{l}}$, respectively. The unit cell is encircled by the dotted line.

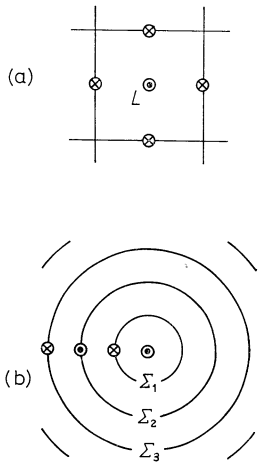

Fig. 3. (a) Type II lattice and (b) concentric structure. The symbols ⊙ and ⊗ denote $\hat{\boldsymbol{l}}$ up and down, respectively.

where $\Phi_L^{(m,n)}$ is the function Φ_L with the singularity in this cell removed (see, (4·6) below), and

$$S_1 - S_2 = 2\Phi_L \,. \tag{3·14}$$

More generally we can add a function analytic in the cell to (3·13) and a periodic function to (3·14). In the following we call this type of structure the non-singular type II lattice. The resulting structure may be regarded as the lattice of A-T structures. We note that the triangular lattice of this type is the one suggested by Volovik and Kopnin.[5]

[b] Concentric sheet structure

Instead of the periodic structure it is also possible to have an entirely different type, a simple example of which is the structure with concentric sheets of the phase discontinuity. For simplicity let us consider concentric circles Σ_n with radius $na\,(n=1, 2, \cdots)$ and put $\chi = n\pi$ on Σ_n (Fig. 3(b)). Since it is clearly necessary that $\partial_\phi S_1 \sim \omega r^2$ and since $S_1+S_2\,(S_1-S_2)$ can be discontinuous on $\Sigma_{2n-1}\,(\Sigma_{2n})$, we suppose

$$S_1(n) = a^2 n^2 \omega\phi \,, \tag{3·15}$$

$$S_2(n) = (-1)^n a^2 n\omega\phi \tag{3·16}$$

between Σ_{n-1} and Σ_n, where ϕ is the polar angle. Because of the single valuedness,

$$a^2\omega = p \,. \tag{3·17}$$

The integrated phase slip of S_1+S_2 (S_1-S_2) on Σ_{2n-1} (Σ_{2n}) is $2\pi(8n-2)$ $(2\pi(8n$

$+2)$). Within Σ_1 we have just the A-T structure. Although the concentric structure seems to be the simplest of this type, one can think of other configurations of the sheets.

§ 4. Estimation of free energy

Since, as we have said before, it is extremely difficult to solve the minimization problem, we try to estimate the free energy of the various types of the structures, assuming simple forms for the functions S_1, S_2 and χ. In all cases of the lattice structure we choose the vortex quantum number $p=1$ since the free energy depends on p^2.

[a·1] In the case of a lattice of ordinary vortex lines the function ζ_0 is given by

$$\zeta_0(Z)=\zeta(Z)+\lambda Z, \tag{4·1}$$

where $Z=X+iY$ and $\zeta(Z)\equiv\zeta(Z;\ (a/2),\ 1/2(b\ \cos\alpha+ib\sin\alpha))$ is the Weierstrass function. The constant λ is determined by the condition

$$\frac{1}{2}a\omega=\zeta\left(\frac{1}{2}a\right)+\lambda\cdot\frac{a}{2} \tag{4·2}$$

to satisfy (3·4). The function Φ_L is obtained as the imaginary part of the integral of ζ_0. We quote the result of Tkachenko's calculation[2] for the energy per area S_κ carrying unit vorticity $\kappa(=h/2m)$;

$$F_{\text{orb}}=\sqrt{2(1+\cos^2\chi)}\frac{\rho_{s\parallel}}{2m^2}\times\begin{cases}-4.117-\pi\ln\xi\sqrt{\dfrac{\omega}{\pi}} & \text{for the square lattice},\\ -4.150-\pi\ln\xi\sqrt{\dfrac{\omega}{\pi}} & \text{for the triangular lattice}.\end{cases} \tag{4·3}$$

Here ξ is the radius of the core which is of the order of the coherence length.

[a·2] Type I lattice. As an example we choose the square lattice shown in Fig. 2. The triangular lattice does not seem to be preferable because each L site is then surrounded by 3 nearest-neighbour C sites instead of 4 in the case of the square lattice. From (3·12) the lattice constant is $d=\sqrt{2\pi/\omega}$. For the purpose of estimation we simply drop S_1' and S_2' in (3·11) and use the square lattice potentials Φ_L and Φ_C. The branch cut is always taken in the positive x direction. For this lattice $\lambda=0$ and it is convenient to use the scale such that $d=1.854\cdots$. In the calculation we make use of the expansion,

$$\Phi_L(x_0,y_0)=\mathrm{Im}\int_0^{z_0}\zeta(z')\,dz'$$

Table I. Free energy of various types of textures per area carrying unit vorticity $(h/2m)$ in the unit of $\rho_{s\parallel}/2(2m)^2$.

		F_{sp}	F_{orb}	F_{total}
Type I Square Lattice	$\delta S_2=0$	47.8	30.6	78.4
	$\delta S_2=\pi/2$	54.9	22.1	77.0
Type II Square Lattice	$\delta S_2=0$	80.9	56.5	137.4
	$\delta S_2=\pi/2$	102.9	28.6	131.5
Type II Triangular Lattice	$\delta S_2=0$	66.9	54.5	121.4
Concentric sheets		113.6	60.7	174.3
M-H Structure	$\delta S_2=0$	40.8	24.3	65.2
	$\delta S_2=\pi/2$	45.2	18.6	63.8
A-T Structure	$\delta S_2=0$	61.8	43.3	105.1
	$\delta S_2=\pi/2$	72.1	21.7	93.8
Singular Vortex Triangular Lattice	$\chi=0$	0	$-25.1\cdot\ln\xi\sqrt{\omega/\pi}-33.2$	

$$= \tan^{-1}\frac{y_0}{x_0}-\frac{1}{60}(x_0^3y_0-x_0y_0^3)$$

$$-\frac{1}{8400}(x_0^7y_0-7x_0^5y_0^3+7x_0^3y_0^5-x_0y_0^7)+\cdots. \qquad (4\cdot4)$$

The function S_1 is obtained as the potential of the square lattice made up of vortex lines at both L and C sites. For the function χ we use

$$\chi(x,y)=\frac{\pi}{2}\left[1-\frac{1}{2}\left(\cos\frac{2\pi x}{d}+\cos\frac{2\pi y}{d}\right)\right] \qquad (4\cdot5)$$

which has the lattice symmetry and is equal to 0 at L and π at C sites. With these functions we have calculated the free energy (2·9) and (2·10), the result of which is presented in Table I. We have also calculated the current density (2·12). The flow pattern is shown in Figs. 4(a) and (b). Note that, because of the bending of $\hat{l}$-vector, we have the z component of the current density though it integrates to zero.

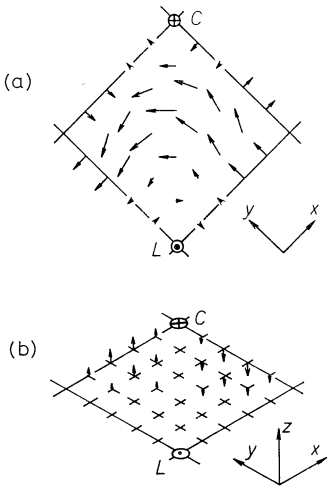

Fig. 4. (a) The projection on the x-y plane and (b) the z-component of the current density in the type I lattice.

[a·3] Type II lattice. Taking the square lattice as above, we use the functions S_1 and S_2

which are given in the (m, n)-th cell by

$$S_1(m, n) = 2\Phi_L - \varphi_{m,n},$$
$$S_2(m, n) = -\varphi_{m,n},$$
$$\chi(x, y) = \pi\left(1 - \cos\frac{\pi x}{2d}\cos\frac{\pi y}{2d}\right), \tag{4·6}$$

where φ_{mn} is the polar angle around the (m, n)-th lattice site measured from the x axis. The result is shown in Table I. We have calculated the energy of the triangular structure also which turns out to be, against our expectation, only slightly lower than that of the square lattice.

[b] Concentric structure. We use S_1 and S_2 in (3·15), (3·16). Since we are interested in the energy proportional to the area, we can neglect terms of $O(1/n)$ in calculating the contribution from the region $na < r < (n+1)a$. If we assume χ to depend only on r, we can perform the φ-integral, after which we find the energy per S_K

$$F_{\rm sp} = \frac{\rho_{s\parallel}}{2(2m)^2}\frac{\pi}{a}\int_0^a dr_0(3+\cos^2\chi)\left[(\chi')^2+\sin^2\chi\right] \tag{4·7}$$

and

$$F_{\rm orb} = \frac{\rho_{s\parallel}}{2(2m)^2}\frac{\pi}{a}\int_0^a dr_0\Big[(1+\sin^2\chi)(\chi')^2+4\left(\frac{r_0}{a}\right)^2(3+\cos^2\chi)$$
$$\pm 16\frac{r_0}{a}\cos\chi+2(1+\cos^2\chi)\Big], \tag{4·8}$$

where $r_0 = r - na$. The signs $\pm$ correspond to n odd and even. If we further assume $\chi = \pi r/a$, we obtain the following results:

$$F_{\rm sp}\Big/\frac{\rho_{s\parallel}}{2(2m)^2} = \frac{7}{2}\pi^3+\frac{13}{8}\pi = 113.6 \tag{4·9}$$

and

$$F_{\rm orb}\Big/\frac{\rho_{s\parallel}}{2(2m)^2} = \frac{3}{2}\pi^3+\frac{23}{3}\pi-\frac{31}{\pi} = 60.7\,. \tag{4·10}$$

§ 5. Discussion

According to the results of the preceding section summarized in Table I the lattice of the non-singular linear structures seems to be the most stable type of texture in the rotating cylinder. Since in the evaluation of the free energy we have used the trial functions and hence the values obtained are the upper bounds, we feel that the relative magnitude of the energy of the three types of the structures will remain the same in the exact calculation. A simple improvement of the

trial functions is merely to add a constant phase δS_2 to S_2 in the case of the type I and II lattices. When $\delta S_2=\pi/2$ we attain the lowest energy listed also in the Table. By adding δS_2 we rotate $\hat{l}$-vector in such a way that the flow $\boldsymbol{v}$ is along $\hat{\boldsymbol{l}}$ in more part of the fluid than before. As a result the energy is lowered due to the anisotropy of ρ_s. We note that a similar improvement is possible for other types of the structures.

Since we may regard our type I lattice as composed of the M-H structures (four of them in a unit cell), it is interesting to compare the energy of the lattice per quarter of the unit cell area with the energy of the M-H structure in a cylinder. In doing this we have to use the free energy of the latter in the frame rotating with angular velocity $\omega=1/R^2$ where the radius R satisfies $\pi R^2=\frac{1}{4}\times$ (the unit cell area). Unlike the M-H structure in the rest frame, it is not possible to solve the minimization problem in this case.*) Since the linear form, $\chi(r)=\frac{1}{2}\pi(r/R)$, is a very good approximation in the rest frame,[9] we also use it here to evaluate the energy in the rotating frame

$$F_{\rm sp}\Big/\frac{\rho_{s\parallel}}{2(2m)^2}=4\pi\int_0^R rdr\Big[(\chi')^2(1+\cos^2\chi)+2\frac{\sin^2\chi}{r^2}\Big],$$

$$F_{\rm orb}\Big/\frac{\rho_{s\parallel}}{2(2m)^2}=2\pi\int_0^R rdr\Big[(\chi')^2(1+2\sin^2\chi)+2\chi'\sin\chi\,\frac{1-\cos\chi}{r}+\frac{\sin^2\chi}{r^2}$$
$$+4\frac{(1-\cos\chi)^2}{r^2}-2\chi'\omega r\sin\chi-8\omega(1-\cos\chi)+4(\omega r)^2\Big]. \qquad (5\cdot1)$$

The numerical results $F_{\rm sp}=40.8$ and $F_{\rm orb}=24.3$ are to be compared with 47.8 and 30.6 of our lattice (Table I). In view of the lower symmetry in the case of the lattice we interpret this to imply that our estimate is not far from the minimum value. Since we need not impose the usual boundary condition at the wall, we can also add $\delta S_2=\pi/2$ so that near the wall of the cylinder $\hat{\boldsymbol{l}}$ is parallel to $\boldsymbol{v}/\!/\hat{\boldsymbol{\varphi}}$. When we do this, the energy of the M-H structure is lowered to $F_{\rm sp}=45.2$, $F_{\rm orb}=18.6$. A similar consideration can be made for the type II lattice structure, the energy of which we compare with the corresponding energy of the A-T structure evaluated in the same way as above (Table I).

There are several remarks to be made.

1) Improvement of the trial functions and the stability of the structures can be studied by the perturbation method. This may be especially interesting in the case of the structure with the sheet singularity.

2) As to the structures with the sheet singularity in the phase functions, we remark that it does not lead to real singularity, i.e., to divergent $\boldsymbol{v}$, provided in the free energy such terms as $(\nabla^2 A_{ij})^2$ are absent. (For the non-singular vortex lattice they will only lead to logarithmic divergence in the energy.) This point may be

*) A similar calculation was made by Soda and Shiwa.[8] However, they used F-$L_s\Omega$ instead of the correct expression F-$L\Omega$, although the difference is immaterial for their purpose.

important in the stability problem.

3) So far we have neglected the effect of the container wall. At both ends of the cylinder our lattice structures will naturally terminate, we expect, with a composite (2-dimensional) lattice of the circular and the hyperbolic boojum. Recently, Hu et al.[10] obtained an approximate solution for the A-T structure confined between two parallel plates and pointed out that, when their distance D becomes sufficiently small, the transition to the uniform texture will take place. According to them the critical value D_{cr} is given by

$$D_{cr} \sim 158 (\xi R)^{1/2},$$

where R is the radius and ξ the coherence length. If we ignore the effect of rotation and simply put $R \sim d \sim \sqrt{\pi\hbar/m\Omega} = 0.026\, \Omega^{-1/2}$ (cm), we get $D_{cr} \sim 0.025$ cm for $\Omega = 1$ rad/sec ($\xi \sim 10^{-6}$ cm).

4) We expect the dipole locking of d- and l-vector will be maintained as long as $d \gg \xi_d$ where ξ_d is the dipole coherence length $\sim 10^{-4}$ cm, hence at any feasible rotation. The effect of a magnetic field, however, should be very interesting and will be discussed elsewhere. We only point out, as an example, that when a magnetic field parallel to the rotation axis is applied, $\hat{\boldsymbol{d}}$ and hence $\hat{\boldsymbol{l}}$ will tend to stay in the x-y plane, thus modifying the orbital texture also.

5) To study these structures experimentally, NMR and ultrasonic attenuation seem to be most suitable. What we should expect in these experiments will also be discussed in future work. We note, however, that fluctuations in the texture could be very large because of the small differences in the energy of the various structures. Therefore, it may be difficult to observe any clear-cut structure in an actual experiment.

This work was partially financed by the Grant-in-Aid for Scientific Research from the Ministry of Education. One of us (T.F.) would like to thank Research Institute for Fundamental Physics, where a part of this work was done, for hospitality extended to him.

References

1) See, for example, N. D. Mermin, *Quantum Liquids* edited by J. Ruvalds and T. Regge, (North-Holland, 1978), p. 195.
2) V. K. Tkachenko, Soviet Phys.-JETP **22** (1966), 1282.
3) N. D. Mermin and T.-L. Ho, Phys. Rev. Letters **36** (1976), 594.
4) P. W. Anderson and G. Toulouse, Phys. Rev. Letters **38** (1977), 508.
5) G. E. Volovik and N. B. Kopnin, Pis. Zh. Eksp. i Teor. Fiz. **25** (1977), 26.
6) T. Tsuneto, T. Ohmi and T. Fujita, *Proceedings of the ULT Hakoné Symposium* (1977), p. 153.
7) V. R. Chechetkin, Soviet Phys.-JETP **44** (1976), 766.
8) T. Soda and Y. Shiwa, *Proceedings of the ULT Hakoné Symposium* (1977), p. 150.
9) K. Maki and T. Tsuneto, J. Low Temp. Phys. **27** (1977), 635.
10) C.-R. Hu, T. E. Ham and W. M. Saslow, preprint.